In Situ Patterning of High-Quality Crystalline Rubrene Thin Films for High-Resolution Patterned Organic Field-Effect Transistors

Hyeok Moo Lee,[†] Jae Joon Kim,[†] Jae Hak Choi,[‡] and Sung Oh Cho[†,*]

[†]Department of Nuclear and Quantum Engineering, Korea Advanced Institute of Science and Technology, Daejeon 305-701, Korea, and [‡]Radiation Research Division for Industry and Environment, Korea Atomic Energy Research Institute, Jeongeup-si, Jeollabuk-do 580-185, Korea

ABSTRACT For the realization of high-performance patterned organic field-effect transistors (OFETs), we present a novel approach to fabricate patterned crystalline rubrene thin films by combining an abrupt heating technique and a lift-off process. Crystallization of rubrene thin films and the patterning of the films are accomplished almost simultaneously and *in situ* by this approach. Consequently, patterned rubrene crystalline films are remarkably rapidly produced within 2 min. High-quality crystalline rubrene patterns with a submicrometer spatial resolution were readily prepared by this approach. OFETs made of submicrometer rubrene crystal wires exhibited mobilities of as high as 4.5 $cm^2 V^{-1} s^{-1}$ at ambient conditions, which is the highest value reported so far of OFETs based on one-dimensional micro/nano-organic semiconductors.

KEYWORDS: organic field-effect transistors · submicrometer pattern · rubrene · organic thin film

Organic field-effect transistors (OFETs) have attracted much attention for their practical applications to a variety of organic electronics.[1−8] Rapid progress in OFETs simultaneously requires both the preparation of high-quality organic semiconductor thin films with a high mobility and the patterning of these organic active layers over a large area with a high spatial resolution of submicrometer level.[9] The patterning of active organic semiconductors in OFETs is a prerequisite to decrease parasitic leakage or crosstalk between neighboring devices. Conventional patterning techniques for inorganic semiconductors, such as lithography, can hardly be used for the patterning of organic semiconductors because organic materials tend to be easily damaged by radiation, energetic particles, and solvents.[10]

Typically, semiconducting oligomers exhibit better OFET performance than polymers.[11] Semiconducting oligomer patterns can be prepared by vacuum deposition using a shadow mask, but this method has a limited spatial resolution.[12] Therefore, several alternative patterning methods have been developed including inkjet printing,[13] vapor jet,[14] soft lithography,[15] direct electron-beam writing,[16] selective crystallization technique,[17] and lift-off process.[18,19] However, these techniques mostly require two different processes for the fabrication of patterned oligomer semiconductors: (1) formation of crystalline oligomer semiconductors and (2) patterning of the organic semiconductors. The patterning process can be followed by the crystallization process, or *vice versa*. These two processes are generally completely separated, and hence a careful sample treatment to prevent oxidation or contamination between the two processes and long times are necessary for the fabrication of patterned active organic semiconducting layers. Moreover, patterned OFETs fabricated using these methods show relatively low carrier mobilities and a low-resolution pattern.

Among organic semiconductors, rubrene shows the highest carrier mobility in the form of single-crystal transistors.[20] However, OFETs with rubrene thin films did not exhibit superior carrier mobilities because of the difficulty in achieving high-quality crystalline rubrene thin layers.[21−23] In our previous study, we reported that continuous, highly ordered, and uniaxially oriented crystalline rubrene thin films comprising large single-crystalline grains could be successfully prepared by an abrupt heating technique.[24] In this study, we report a straightforward strategy to fabricate patterned crystalline rubrene thin films for high-performance patterned OFETs. The formation of high-quality crystalline rubrene thin films and the patterning of the crystalline rubrene films are accomplished

* Address correspondence to socho@kaist.ac.kr.

Received for review August 11, 2011 and accepted September 17, 2011.

Published online September 17, 2011
10.1021/nn203068q

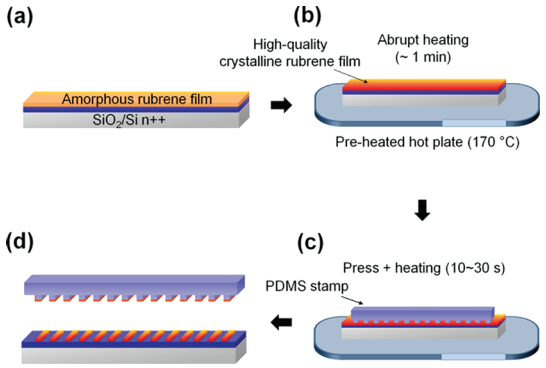

Figure 1. Schematic illustration of the fabrication of the patterned crystalline rubrene thin films using a PDMS lift-off process.

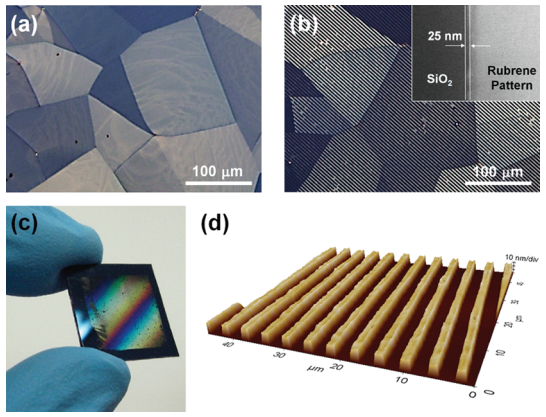

Figure 2. POM images of the (a) crystalline rubrene thin films fabricated by an abrupt heating process at 170 °C for 1 min and (b) array of crystalline rubrene microwires with equal line width and space of 2 μm. The inset of (b) is the SEM image that shows the edge of a microwire, which indicates that edge roughness of rubrene microwires is about 25 nm. (c) Optical image showing interference fringes of the rubrene microwire array on an area of 1.5 cm × 1.5 cm. (d) Three-dimensional AFM image of the crystalline rubrene patterns.

almost simultaneously and *in situ* by combining the abrupt heating technique and a lift-off process. The patterned rubrene crystalline films are remarkably rapidly produced: the total process time for both the crystallization and the patterning is less than 2 min. Through this *in situ* method, micrometer and submicrometer scale crystalline rubrene wire arrays and submicrometer OFET devices were demonstrated. To the best of our knowledge, this is the first report to pattern crystalline rubrene thin films with a submicrometer spatial resolution. Moreover, the OFETs made of the rubrene submicrometer wires exhibited the saturation mobilities of as high as 4.5 $cm^2\ V^{-1}\ s^{-1}$ at ambient conditions, which is the highest value reported so far of OFETs based on one-dimensional (1D) micro/nano-organic semiconductors.[25,26]

RESULTS AND DISCUSSION

The schematic representation for the fabrication process of the patterned crystalline rubrene films is shown in Figure 1. An amorphous rubrene film is prepared on a SiO_2 dielectric layer by thermal evaporation (Figure 1a). The amorphous rubrene film is directly transformed into a crystalline rubrene thin film by an abrupt heating process,[24] which was carried out by placing an as-deposited rubrene film on a preheated hot plate in a dark room at 170 °C for 1 min (Figure 1b). The polarized optical microscopy (POM) image of the produced crystalline rubrene thin film reveals that a continuous crystalline film consisting of large-sized (average size = ~80 μm) and well-faceted domains was created over the whole dielectric surfaces (Figure 2a). Two-dimensional grazing-incidence X-ray diffraction (2D GIXD) pattern reveals that the film consists of highly ordered rubrene crystals and that the *c* axes of the crystals are aligned perpendicular to the substrate surface, while *ab* planes of the crystals are perfectly oriented parallel to the substrate surface (Figure S1 in the Supporting Information).[27] In addition, no color variation was observed within a single domain under POM investigation, suggesting that a domain is composed of a single-crystalline grain.[28]

TABLE 1. Contact Angle (deg) and Surface Energy (mJ m^{-2}) of SiO_2, PDMS, and Crystalline Rubrene Film[a]

	contact angle				
	water	ethylene glycol	γ_s^d	γ_s^p	γ_s
SiO_2	47	31	7.65	46.46	54.11
PDMS	92	70	18.58	4.01	22.59
crystalline rubrene film	90	59	32.42	1.48	33.90

[a] The γ_s^d and γ_s^p are the dispersion and polar components of the surface energy, respectively, and γ_s is the surface energy ($\gamma_s = \gamma_s^d + \gamma_s^p$).

During the abrupt heating process for the crystallization, a prepatterned PDMS stamp is pressed onto the rubrene film with a low pressure of ~130 g cm^{-2} for 10−30 s while keeping the temperature at 170 °C (Figure 1c). Thereafter, the sample is taken out of the hot plate, and the stamp is separated from the film. When the stamp is detached, rubrene materials contacting with the stamp are removed from the substrate, while noncontacted rubrene materials remain on the substrate. As a consequence, a patterned crystalline rubrene film is fabricated (Figure 1d). This lift-off process is generally attributed to the difference in the work of adhesion between two interfaces.[18] The work of adhesion at the interfaces of rubrene/SiO_2 ($W_{rubrene/SiO_2}$) and the rubrene/PDMS stamp ($W_{rubrene/PDMS}$) was evaluated by contact angle measurements using water and ethylene glycol at room temperature.[29] The corresponding contact angle and the surface energy of each surface derived from the measurements are given in Table 1, and the estimated work of adhesion is $W_{rubrene/SiO_2}$ = 30.49 mJ m^{-2} and $W_{rubrene/PDMS}$ = 51.57 mJ m^{-2}. The value of $W_{rubrene/PDMS}$ is larger than $W_{rubrene/SiO_2}$, and thus, if a rubrene

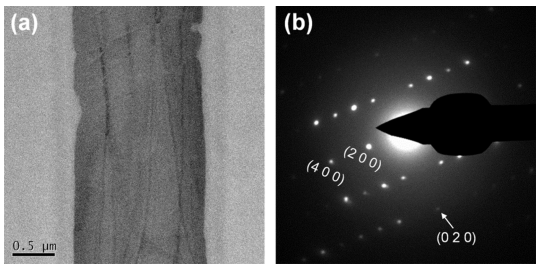

Figure 3. (a) TEM images of the crystalline rubrene microwire fabricated on SiO_2-coated TEM grid and (b) corresponding SAED patterns. The SAED pattern was recorded along the [001] zone axis of the orthorhombic rubrene.

film on SiO_2 is pressed with a PDMS stamp, the rubrene materials contacting the stamp are transferred to the stamp. However, we observed that clear rubrene patterns were fabricated only at a temperature higher than 160 °C (Figure S2), and that crystalline rubrene materials were not lifted off at all at room temperature even though a PDMS stamp was pressed with a much higher pressure than needed at the optimum temperature of ~170 °C. On the basis of previous literature, we can conclude that elevated temperature is essential for obtaining intimate contact and enhanced adhesion between the stamp and the rubrene film, facilitating the transfer of the rubrene film from the substrate to the stamp.[18,30,31] Therefore, the lift-off patterning process can be carried out almost simultaneously during the crystallization process of rubrene thin films at 170 °C, allowing the *in situ* patterning of crystalline rubrene thin films.

We note that patterned crystalline rubrene films are very rapidly fabricated through our approach presented here: the total process time for the crystallization and the patterning is only 2 min. Additionally, the produced rubrene patterns consist of very high-quality rubrene crystals, and crystalline rubrene patterns with a high spatial resolution can be readily prepared by controlling the pattern size of a PDMS stamp. Figure 2b–d shows the representative results of the patterned crystalline rubrene films fabricated by the approach. An array of microwires with the uniform width of 2 μm, thickness of 20 nm, and spacing of 2 μm was formed over an area of 1.5 cm × 1.5 cm. The POM and atomic force microscope (AFM) images (Figure 2b,d) show that exquisite patterns without any residual material remaining on the SiO_2 dielectrics were achieved. The crystalline nature of the produced rubrene microwires was characterized with a transmission electron microscope (TEM). The length of the microwires (approximately a few millimeters) is much larger than the average domain size (~80 μm), and thus, a single microwire is formed over many crystal domains. However, the microwire in a domain is a single crystal because a domain is composed of a single-crystalline grain. The single

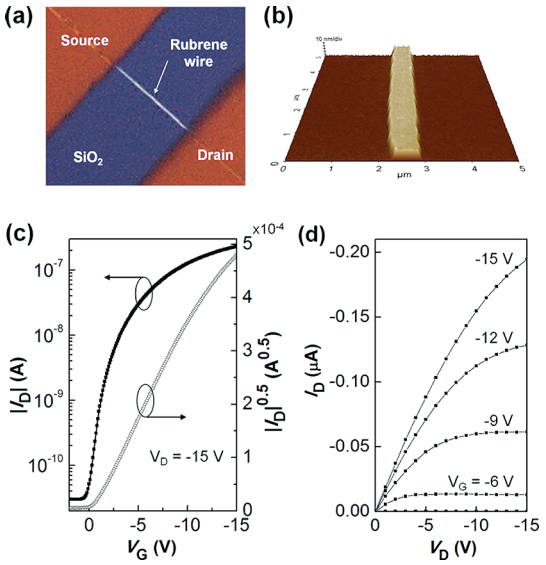

Figure 4. (a) POM images of the crystalline submicrometer rubrene wire channel. (b) Magnified three-dimensional AFM image of the corresponding active channel in (a). (c) Drain current (I_D) and square root of the drain current *versus* gate voltage (V_G) at a drain–source voltage of −15 V. (d) Drain current *versus* drain voltage characteristics for various gate voltages (V_D).

crystallinity of a microwire in a domain was verified by selected area electron diffraction (SAED) patterns. The SAED pattern in Figure 3b clearly displays a set of sharp and regular spots, and the pattern was indexed to an orthorhombic rubrene single-crystalline phase.[24]

To demonstrate the effectiveness of our strategy, OFET devices were fabricated with the patterned crystalline rubrene films. For the devices, isolated crystalline rubrene wires with a width of 650 nm and a thickness of 20 nm were produced using the same technique for the microwires fabrication (Figure 4a,b). Gold source and drain electrodes were prepared on these rubrene submicrometer wires *via* vacuum deposition. The channel length of the submicrometer OFET is 32 μm. As shown in Figure 2a,b, the average size of a domain in the crystalline rubrene film is ~80 μm, which is sufficiently larger than the channel length of the device. Hence, OFETs based on single-crystalline rubrene submicrometer wires could be fabricated if both the source and drain electrodes were prepared in the same domain (Figure S4a). The POM image (Figure 4a) of the rubrene submicrometer wire channel in the OFET displays no color variation along the wire axis, confirming the single-crystalline nature of the rubrene wire. As can be expected, OFETs made of the single-crystalline rubrene submicrometer wires exhibited very high performance. The representative transfer and output characteristics of the fabricated FETs are shown in Figure 4c,d. The hole mobility, extracted from the saturation regime at a drain–source voltage (V_D) of −15 V, was as high as 4.5 $cm^2\ V^{-1}\ s^{-1}$ at ambient conditions. This value is the

highest mobility ever reported for OFETs made of 1D, such as wires and ribbons, organic micro/nanostructures. The threshold voltages deduced by the linear extrapolation of the saturation region in the square root of the drain current *versus* gate voltage were as small as 0.22 V. The on/off current ratio was about 10^4. From the random test of seven devices, the OFETs based on the rubrene submicrometer wires had charge mobilities ranging from 1.6 to 4.5 $cm^2\ V^{-1}\ s^{-1}$. This variation of the mobility is mainly attributed to the anisotropic charge transport behavior of a rubrene single crystal:[20] the crystallographic *a* and *b* axes are randomly oriented in the rubrene submicrometer wires, and hence the mobility along the submicrometer wire axis has a variation (see details in Supporting Information, Figures S3 and S4). In addition, an OFET can be occasionally produced with a submicrometer wire formed over two neighboring domains (Figure S4biii), and then a grain boundary exists inside the wire channel. Nevertheless, it should be noted that the OFET devices made of the submicrometer rubrene wires show a state-of-the-art performance of OFETs based on 1D organic semiconductors, reflecting the excellence of our *in situ* approach for the fabrication of patterned high-quality crystalline rubrene thin films.

CONCLUSIONS

In summary, we have presented a simple but effective approach to fabricate patterned crystalline rubrene active layers for high-performance patterned OFETs. By combining an abrupt heating process for the crystallization of rubrene thin films and a lift-off process for the patterning of the rubrene thin films, patterned crystalline rubrene thin films can be readily fabricated *in situ*. Since the two processes are carried out almost simultaneously and *in situ*, patterned crystalline rubrene thin films can be remarkably rapidly fabricated within 2 min. The produced rubrene thin films have very high crystalline quality, and a pattern with a submicrometer spatial resolution can be controllably prepared by this route. Moreover, submicrometer OFETs fabricated based on this approach exhibited excellent performance. Therefore, we believe that our approach is very promising for the practical applications to a variety of organic electronic and optical devices.

EXPERIMENTAL SECTION

The formation process of the crystalline rubrene thin films using an abrupt heating process was described in detail in our previous report.[24] Briefly, amorphous rubrene thin films were thermally deposited on 100 nm thick SiO_2 dielectric surfaces underlying heavily doped n-type silicon substrates (2 cm × 2 cm), and then the as-deposited rubrene thin films were abruptly heated by placing the samples onto a hot plate preheated at 170 °C in a nitrogen-filled glovebox. PDMS stamps were prepared by casting PDMS resin (Sylgard 184, Dow Corning) and curing agent at a 10:1 weight ratio against the patterned silicon master mold. After curing at 80 °C for 1 h, the elastomer stamp was carefully released from the mold.

The surface energy and interfacial energy associated with PDMS, SiO_2, and crystalline rubrene film were analyzed by contact angle measurements using water and ethylene glycol (Phoenix 300, Surface Electro Optics). POM images were captured using an Olympus BX51 microscope. The topographies and the thicknesses of the films were examined with an AFM (XE-70, Park Systems) and a field-emission scanning electron microscope (SEM) (Hitachi S-4800). The TEM images and SAED patterns were taken with a Tecnai G2 Spirit BioTWIN TEM (FEI Company) operating at 120 kV. For TEM observation, patterned rubrene films were prepared on SiO_2-coated TEM grids using the same abrupt heating method and PDMS stamp. GIXD measurements were performed using the 4C2 beamline at the Pohang Accelerator Laboratory (PAL), Pohang, Korea. The diffraction patterns were recorded using a MarCCD detector. The grazing-incidence angle of the X-ray beam (λ = 1.3807 Å) was varied between 0.14 and 0.25°; the sample-to-detector distance (143.5 mm) was calibrated using a silver behanate standard sample, and the footprint of the X-ray beam on the specimen surface was 1 mm × 5 mm. The diffraction data were displayed as an intensity map in which q_{xy} is the in-plane momentum transfer and q_z is the out-of-plane momentum transfer. The OFET characteristics were evaluated using a probe station (Semiconductor Characterization System 4200 SCS/F and Summit 11862B, Keithley and Cascade) under ambient conditions. The carrier motilities were extracted in the saturation regime using the equation based on parallel-plate model, $I_D = \mu C_i(W/2L)(V_G - V_T)^2$, where I_D is the drain current, C_i is the capacitance per unit area of the gate dielectric layer (C_i = 34.5 nF/cm^2), and V_G is the gate bias voltage.

Acknowledgment. This work was supported by the National Research Foundation (NRF) of Korea grant funded by the Korea Ministry of Education, Science and Technology (MEST) (No. 2011-0020764).

Supporting Information Available: Two-dimensional GIXD patterns of the crystalline rubrene thin films, SAED patterns of the rubrene microwires, POM, SEM, and AFM images of the array of crystalline rubrene microwires obtained at various lift-off conditions. This material is available free of charge *via* the Internet at http://pubs.acs.org.

REFERENCES AND NOTES

1. Smits, E. C. P.; Mathijssen, S. G. J.; van Hal, P. A.; Setayesh, S.; Geuns, T. C. T.; Mutsaers, K.; Cantatore, E.; Wondergem, H. J.; Werzer, O.; Resel, R.; *et al.* Bottom-Up Organic Integrated Circuits. *Nature* **2008**, *455*, 956–959.
2. Crone, B.; Dodabalapur, A.; Lin, Y. Y.; Filas, R. W.; Bao, Z.; LaDuca, A.; Sarpeshkar, R.; Katz, H. E.; Li, W. Large-Scale Complementary Integrated Circuits Based on Organic Transistors. *Nature* **2000**, *403*, 521–523.
3. Rotzoll, R.; Mohapatra, S.; Olariu, V.; Wenz, R.; Grigas, M.; Dimmler, K.; Shchekin, O.; Dodabalapur, A. Radio Frequency Rectifiers Based on Organic Thin-Film Transistors. *Appl. Phys. Lett.* **2006**, *88*, 123502.
4. Gelinck, G.; Heremans, P.; Nomoto, K.; Anthopoulos, T. D. Organic Transistors in Optical Displays and Microelectronic Applications. *Adv. Mater.* **2010**, *22*, 3778–3798.
5. Sekitani, T.; Nakajima, H.; Maeda, H.; Fukushima, T.; Aida, T.; Hata, K.; Someya, T. Stretchable Active-Matrix Organic Light-Emitting Diode Display Using Printable Elastic Conductors. *Nat. Mater.* **2009**, *8*, 494–499.

6. Gundlach, D. J. Low Power, High Impact. *Nat. Mater.* **2007**, *6*, 173–174.
7. Martinez, M. T.; Tseng, Y. C.; Ormategui, N.; Loinaz, I.; Eritja, R.; Bokor, J. Label-Free DNA Biosensors Based on Functionalized Carbon Nanotube Field Effect Transistors. *Nano Lett.* **2009**, *9*, 530–536.
8. Someya, T.; Sekitani, T.; Iba, S.; Kato, Y.; Kawaguchi, H.; Sakurai, T. A Large-Area, Flexible Pressure Sensor Matrix with Organic Field-Effect Transistors for Artificial Skin Applications. *Proc. Natl. Acad. Sci. U.S.A.* **2004**, *101*, 9966–9970.
9. Briseno, A. L.; Mannsfeld, S. C. B.; Ling, M. M.; Liu, S. H.; Tseng, R. J.; Reese, C.; Roberts, M. E.; Yang, Y.; Wudl, F.; Bao, Z. N. Patterning Organic Single-Crystal Transistor Arrays. *Nature* **2006**, *444*, 913–917.
10. Menard, E.; Meitl, M. A.; Sun, Y.; Park, J. U.; Shir, D. J. L.; Nam, Y. S.; Jeon, S.; Rogers, J. A. Micro- and Nanopatterning Techniques for Organic Electronic and Optoelectronic Systems. *Chem. Rev.* **2007**, *107*, 1117–1160.
11. Facchetti, A. Semiconductors for Organic Transistors. *Mater. Today* **2007**, *10*, 28–37.
12. Baude, P. F.; Ender, D. A.; Haase, M. A.; Kelley, T. W.; Muyres, D. V.; Theiss, S. D. Pentacene-Based Radio-Frequency Identification Circuitry. *Appl. Phys. Lett.* **2003**, *82*, 3964–3966.
13. Lim, J. A.; Lee, W. H.; Lee, H. S.; Lee, J. H.; Park, Y. D.; Cho, K. Self-Organization of Ink-Jet-Printed Triisopropylsilylethynyl Pentacene *via* Evaporation-Induced Flows in a Drying Droplet. *Adv. Funct. Mater.* **2008**, *18*, 229–234.
14. Shtein, M.; Peumans, P.; Benziger, J. B.; Forrest, S. R. Direct, Mask- and Solvent-Free Printing of Molecular Organic Semiconductors. *Adv. Mater.* **2004**, *16*, 1615–1620.
15. Serban, D. A.; Greco, P.; Melinte, S.; Vlad, A.; Dutu, C. A.; Zacchini, S.; Iapalucci, M. C.; Biscarini, F.; Cavallini, M. Towards All-Organic Field-Effect Transistors by Additive Soft Lithography. *Small* **2009**, *5*, 1117–1122.
16. Gibbons, F. P.; Manickam, M.; Preece, J. A.; Palmer, R. E.; Robinson, A. P. G. Direct Electron-Beam Writing of Highly Conductive Wires in Functionalized Fullerene Films. *Small* **2009**, *5*, 2750–2755.
17. Di, C. A.; Yu, G.; Liu, Y.; Guo, Y.; Sun, X.; Zheng, J.; Wen, Y.; Wu, W.; Zhu, D. Selective Crystallization of Organic Semiconductors for High Performance Organic Field-Effect Transistors. *Chem. Mater.* **2009**, *21*, 4873–4879.
18. Wang, Z.; Zhang, J.; Xing, R.; Yuan, J.; Yan, D.; Han, Y. Micropatterning of Organic Semiconductor Microcrystalline Materials and OFET Fabrication by "Hot Lift Off". *J. Am. Chem. Soc.* **2003**, *125*, 15278–15279.
19. Kim, K. H.; Bong, K. W.; Lee, H. H. Alternative to Pentacene Patterning for Organic Thin Film Transistor. *Appl. Phys. Lett.* **2007**, *90*, 093505.
20. Sundar, V. C.; Zaumseil, J.; Podzorov, V.; Menard, E.; Willett, R. L.; Someya, T.; Gershenson, M. E.; Rogers, J. A. Elastomeric Transistor Stamps: Reversible Probing of Charge Transport in Organic Crystals. *Science* **2004**, *303*, 1644–1646.
21. Luo, L.; Liu, G.; Huang, L. W.; Cao, X. Q.; Liu, M.; Fu, H. B.; Yao, J. N. Solution-Based Patterned Growth of Rubrene Nanocrystals for Organic Field Effect Transistors. *Appl. Phys. Lett.* **2009**, *95*, 263312.
22. Li, Z. F.; Du, J.; Tang, Q.; Wang, F.; Xu, J. B.; Yu, J. C.; Miao, Q. A. Induced Crystallization of Rubrene in Thin-Film Transistors. *Adv. Mater.* **2010**, *22*, 3242–3246.
23. Park, S. W.; Hwang, J. M.; Choi, J. M.; Hwang, D. K.; Oh, M. S.; Kim, J. H.; Ima, S. Rubrene Thin-Film Transistors with Crystalline and Amorphous Channels. *Appl. Phys. Lett.* **2007**, *90*, 153512.
24. Lee, H. M.; Moon, H.; Kim, H.-S.; Kim, Y. N.; Choi, S.-M.; Yoo, S.; Cho, S. O. Abrupt Heating-Induced High-Quality Crystalline Rubrene Thin Films for Organic Thin-Film Transistors. *Org. Electron.* **2011**, *12*, 1446–1453.
25. Tang, Q.; Jiang, L.; Tong, Y.; Li, H.; Liu, Y.; Wang, Z.; Hu, W.; Liu, Y.; Zhu, D. Micrometer- and Nanometer-Sized Organic Single-Crystalline Transistors. *Adv. Mater.* **2008**, *20*, 2947–2951.
26. Zhou, Y.; Lei, T.; Wang, L.; Pei, J.; Cao, Y.; Wang, J. High-Performance Organic Field-Effect Transistors from Organic Single-Crystal Microribbons Formed by a Solution Process. *Adv. Mater.* **2010**, *22*, 1484–1487.
27. Yang, H. C.; Shin, T. J.; Ling, M. M.; Cho, K.; Ryu, C. Y.; Bao, Z. N. Conducting AFM and 2D GIXD Studies on Pentacene Thin Films. *J. Am. Chem. Soc.* **2005**, *127*, 11542–11543.
28. Luo, Y.; Gustavo, F.; Henry, J. Y.; Mathevet, F.; Lefloch, F.; Sanquer, M.; Rannou, P.; Grevin, B. Probing Local Electronic Transport at the Organic Single-Crystal/Dielectric Interface. *Adv. Mater.* **2007**, *19*, 2267–2273.
29. Wu, S. H. Polar and Nonpolar Interactions in Adhesion. *J. Adhes.* **1973**, *5*, 39–55.
30. Choi, J.-H.; Kim, D.; Yoo, P. J.; Lee, H. H. Simple Detachment Patterning of Organic Layers and Its Application to Organic Light-Emitting Diodes. *Adv. Mater.* **2005**, *17*, 166–171.
31. Wang, Z.; Yu, X.; Xing, R.; Han, Y.; Takahara, A. Micropatterning of Polymeric Semiconductor by Selective Lift-Off Method Using Epoxy Mold. *J. Vac. Sci. Technol., B* **2009**, *27*, 1958–1962.